SECONDARY FLOW IN NON-CIRCULAR DUCTS

BY

ISLAM OTHMAN MOHAMED GHAFEER
B.Sc. Mechanical Power Engineering,
Faculty of Engineering (Shoubra), Benha University

A Thesis Submitted to the Faculty of
Engineering at Benha University in Partial
Fulfilment of the Requirements for the
Degree of MASTER OF SCIENCE

In

MECHANICAL POWER ENGINEERING

FACULTY OF ENGINEERING (SHOUBRA),
BENHA UNIVERSITY
2014

SECONDARY FLOW IN NON-CIRCULAR DUCTS

BY

ISLAM OTHMAN MOHAMED GHAFEER
B.Sc. Mechanical Power Engineering,
Faculty of Engineering (Shoubra), Benha University

A Thesis Submitted to the Faculty of

Engineering at Benha University in Partial

Fulfilment of the Requirements for the

Degree of MASTER OF SCIENCE

In

MECHANICAL POWER ENGINEERING

Under Supervision of:

Prof. Dr. M. G. HEGAZY **Prof. Dr. OSAMA E. ABDELLATIF**

Prof. Dr. A. M. OTHMAN

Mechanical Power Engineering Department
Shoubra Faculty of Engineering
Benha University

FACULTY OF ENGINEERING (SHOUBRA),
BENHA UNIVERSITY
2014

SECONDARY FLOW IN NON-CIRCULAR DUCTS

BY

ISLAM OTHMAN MOHAMED GHAFEER
B.Sc. Mechanical Power Engineering,
Faculty of Engineering (Shoubra), Benha University

A Thesis Submitted to the Faculty of

Engineering at Benha University in Partial

Fulfilment of the Requirements for the

Degree of MASTER OF SCIENCE

In

MECHANICAL POWER ENGINEERING

Approved by the Examining Committee

Prof. Dr. Essam Khalil Hassan Khalil	Member
Prof. Dr. M. Fayek Abd-Rabbo	Member
Prof. Dr. Maher Gameel Hegazy	Thesis Advisors and Member
Prof. Dr. Osama Ezzat Abdel-Latif	Thesis Advisors and Member
Prof. Dr. Ahmed Maged Othman	Thesis Advisors

SHOUBRA FACULTY OF ENGINEERING, BENHA UNIVERSITY
CAIRO, EGYPT
2014

ABSTRACT

This thesis considers the prediction of turbulence in complex flows using Reynolds Stress Model (RSM). The time evolution of the flow in the square ducts is simulated, and the turbulence-driven secondary flow are predicted in the case of the square duct. Results are compared to both experimental and CFD data. The mean secondary flow structures in the square duct indicate the existence of strong, counter rotating vortex pairs, which are symmetrically placed around the four outer corners of the inner square duct .The additive multigrid method is used to accelerate the convergence of the pressure Poisson equation and the appropriateness of this method to deal with the high wave number components in turbulence is considered. Parallel computing techniques are applied to assist in the solution of the Navier-Stokes equations.

This study is carried out using computational fluid dynamics (CFD) simulation techniques as embedded in the commercially available CFD code (FLUENT 6.2). The CFD modelling techniques solved the continuity, momentum and energy conservation equations.

Throughout the investigations, numerical validation is carried out by way of comparisons of numerical results obtained from FLUENT to results reported in the work of other researcher. Good agreement is found among both predictions.

ACKNOWLEDGEMENT

I wish to express my sincere appreciation and deep gratitude and thanks to Prof. Dr. Osama Ezzat Abdel-Latif for their support, continuous encouragement and distinctive supervision throughout the course of this work. They helped providing me with up to date technical references that were of great help in the present work

Also, I cannot express; in words; my thanks and gratitude to my family for their great and continuous help and support they provided me to finish this work in a suitable form.

Furthermore, deep thanks go to my lovely wife *Aliaa* for her continued support and appreciation during finalizing this thesis.

Sincere thanks are going to my colleagues in the Mechanical Power Engineering department as well as from my Professors for their encouragement and concern throughout the scope of the work.

Finally, I should express my gratitude for the FLUENT® personnel for their kind interest in the current project and their support via supplying us with a free license of the FLUENT® 6.2 CFD package.

CONTENTS

LIST OF FIGURES

LIST OF TABELS

SYMBOLS AND ABBREVIATIONS

NOMENCLATURE

$\bar{u}_i$	Mean velocity
x_i	x-axis position
y_i	y-axis position
z_i	y-axis position
T	Time
$\bar{p}$	Mean pressure
R_{ij}	Reynolds stress tensor
$\acute{u}_i$	i^{th} fluctuation velocity component in x-direction
$\acute{v}_i$	i^{th} fluctuation velocity component in y-direction
$\acute{w}_i$	i^{th} fluctuation velocity component in z-direction
$\widehat{U}_i$	instantaneous velocity in the x_i direction
$\widehat{U}_j$	instantaneous velocity in the x_j direction
C_1 C_2	Empirical constants
K	Fluctuation kinetic energy
$\overline{\acute{v}^2}$	Normal component of turbulence intensity
$\overline{\acute{u}^2}$	Mean square axial fluctuation velocity component
$\sqrt{\overline{\acute{v}^2}}$	Quadratic variation
D_h	Duct hydraulic diameter
$\widehat{P}$	Instantaneous Pressure
ξ	Vorticity
$\overline{\acute{u}\acute{v}}$, $\overline{\acute{v}\acute{\omega}}$, $\overline{\acute{u}\acute{\omega}}$	Turbulent shear stresses
m	Mass of the fluid
F	Force exerted on or by the fluid
A	Area of control surface
dA	Element of Area
$\forall$	Volume of control volume
$d\forall$	Element of volume
V_n	Component of velocity perpendicular to the surface

ρ	Density
B	Net mass flow out of control volume through surface A
C	Time rate of decrease of mass inside control volume ~~V~~
a	Acceleration
G	Net rate of momentum out of control volume across surface A
H	Time rate of change of momentum due to unsteady fluctuation of flow properties inside ~~V~~
f	Net body force per unit mass exerted on the fluid inside ~~V~~
T	Stress tensor due to surface force
I	Unit tensor
τ	Viscous shear stress
τ^L	Laminar stress tensor corresponding to time –averaged turbulent kinematics.
τ^R	Turbulent Reynolds stress tensor which is function of turbulent velocity fluctuations.
$(\nabla V)^T$	The transpose of the matrix form of (∇V)
μ_v	Bulk viscosity
μ	Viscosity
λ	Second coefficient of viscosity
e_i , e_j	Unit vectors
δ_{ij}	The Kronecker delta
W	Conserved variable
f	The component of the convective or diffusive flux vector in the direction normal to CV face
f_e	Value of flux f at cell face center "e"
f_{ne}	Value of flux f at corner ne
f_{se}	Value of flux f at corner se
g_1 , g_2	Coefficients
V	Velocity vector
g_x,g_y,g_z	Ground acceleration in x, y, and z directions
u, v, w	Three orthogonal component of velocity, in x, y, and z direction respectively
σ_{xx} , σ_{yy} , σ_{zz}	Normal stress components
p	Static pressure at point in the fluid
V_i	Velocity component
$\emptyset$	Instantaneous value of a fluid property
$\overline{\emptyset}$	Mean value of the same fluid property
$\acute{\emptyset}$	Fluctuation of the same fluid property
$\bar{\tau}_{ij}$	Mean viscous stress tensor components

τ_{ij}^{R}	Reynolds-stress tensor
K	Turbulent kinetic energy
$\bar{S}_{ij}$	Reynolds-averaged strain-rate tensor
μ_t	turbulence or eddy kinematic viscosity
$\overline{\Omega}_{ij}$	Rotation-rate tensor "Antisymmetric part of the velocity gradient tensor"
σ_k	Turbulent Prandtl number
ε	Dissipation of kinetic energy
$C_\mu, C_{\varepsilon 1}, C_{\varepsilon 2}$	Constants of velocity-field turbulent model
$D_{T,ij}$	Turbulent Diffusive Transport
ϕ_{ij}	pressure-strain term
G_{ij}	Buoyancy on Turbulence

GREEK LETTERS

Δ	Element interval – Change interval of any property
∇	Gradient
ρ	Density, kg/m3
μ	Molecular viscosity, kg/m.s
τ	Shear Stress, kg/m.s2
ϕ	Dissipation function
φ	Donates scalar property (i.e. density, temperature, ..etc.)
ε	Turbulence dissipation rate m2/s3
ω	Vorticity
δ	Boundary layer thickness
β	Thermal expansion coefficient, K-1
κ	Von Kármán constant
Γ	Diffusion coefficient

SUPERSCRIBTS AND SUBSCRIBTS

$\overline{\square}$	Mean property
$\acute{\square}$	Fluctuating component of any property
$\square_{eff}$	Effective property
$\square_{i,j,k}$	Donates Cartesian coordinate direction takes the value of axis x, y, z
$\square_{i}$	Inlet
$\square_{T}$	Time

$\square_{\tau}$	Turbulent property
$\square_{v}$	Viscous
$\square_{w}$	Wall

ABBREVIATIONS

2-D	Two dimensional configurations
3-D	Three dimensional configurations
CFD	Computational Fluid Dynamics
LES	Large Eddy Simulation
PMV	Predicted Mean Vote
PPD	Percentage Predicted Dissatisfied
RNG	Renormalization Group
RSM	Reynolds Stress Model
SST	Shear Stress Transport

CHAPTER ONE

Introduction

1.1 The Problem Considered

The Majority of flows which occur in nature or in engineering practice is turbulent and, more often than not, is three dimensional. One example is the turbulent flow in a duct of non-circular cross-section which is characterized by the existence of secondary motions in the plane normal to the streamwise direction, a feature that is absent from both Laminar and two dimensional flow.

The turbulence structure of internal flows within circular pipes or non-circular ducts can be altered considerably by the occurrence of secondary flows [1-21]. These secondary flows lead to friction losses and can shift the location of maximum momentum transport from the pipe or duct centerline two effects that can have profound consequences for engineering design. Consequently, there is the need for turbulence models that can reliably predict the secondary flows that occur in engineering applications which include turbomachinery impellers and blade passages, aircraft intakes, and pipe or duct cooling systems.

There are four fundamental types of secondary flows: (1) turbulence-driven secondary flows in straight ducts of non-circular cross-section, (2) turbulent secondary flows in curved circular pipes, (3) turbulent secondary flows in curved ducts of non-circular cross-section and (4) turbulent secondary flows in rotating ducts of noncircular cross-section. These flows are selected since they involve secondary flows generated by a combination of the effects of normal Reynolds stress differences, streamline curvature and body forces arising from a system rotation. Thus, a relatively broad basis for the evaluation of models can be provided. The ability of two-equation models and second-order closures to predict these types of turbulent secondary flows will be evaluated in a systematic manner. A variety of illustrative calculations of secondary flows will be presented along with an assessment of the progress that has been made in the analysis of these flows.

The flow in a streamwise corner is considered. It is a three-dimensional turbulent flow bounded by two walls, which may be straight or curved. This type of flow can be external as well

as internal and occurs in many practical applications. The flow around blade-hub junctions and wingbody junctions are examples of external streamwise corner flow. The flow in long ducts and channels fall under the category of internal streamwise corner flows. All of these flows are characterized by the development or decay of streamwise vorticity which alters the primary flow field.

Alternatively, there exists a secondary flow which is superimposed on the primary streamwise flow. Secondary motion in internal flows is important in a variety of engineering applications. For example, the pressure drop in developing or fully-developed flow in duct bends affects the pumping power needed. The heat transfer is enhanced by the secondary motions in the cooling coils of heat exchangers. The flow in aircraft-engine intakes and heat transfer in turbomachinery components are also affected by secondary motion. River meanders and variations in bend topology are induced by secondary motion. In blood flow, the length required for fully-developed flow after a bifurcation and the site of extrema in the wall shear stress are important in the understanding of the buildup of cholesterol on the vessel walls. In external flows, secondary motion arises in three-dimensional boundary layers and in boundary regions such as wing tips and wing-body junctions. While conventional boundary-layer theory accounts for the former, it excludes boundary regions where the surface curvature is either discontinuous, as in corners between two walls, or not small compared with boundary-layer thickness, as in the flow around wing tips and in corners with fillets. The flow in a corner is of special interest since it provides the boundary conditions for the boundary-layer flow in regions remote from the corner. Practical applications arise in wingfuselage junctions in aerodynamics, hull-appendage junctions in ship hydrodynamics, and blade-hub junctions in turbomachinery. The formation and decay of the longitudinal vortices in corners, and the possibilities of corner-flow separation, are phenomena of particular interest in these applications.

Prandtl (1952) classified secondary flows according to the mechanism which generates them. Pressure-driven secondary flow, or secondary flow of the first kind, is that which results from the radial pressure gradients which balance the centrifugal acceleration due to the curvature of the streamlines. Such secondary flows arise in curved ducts and channels, wing-body junctions as well as in turbomachinery. The secondary flow in three-dimensional laminar and turbulent boundary layers is primarily of this type. The magnitude of the secondary flow thus

depends on the curvature of the mean streamlines. Another type of secondary flow, called secondary flow of the second kind, occurs only in turbulent flow and is generated by the gradients of the Reynolds stresses. This is also called shear-driven or turbulence-driven secondary flow. In straight noncircular ducts and channels, the secondary-flow velocities due to this mechanism are usually small, of the order of 2 to 3 percent of the average velocity. In turbulent flow in curved ducts and channels, both types of secondary motion is present but, if the curvature is large, secondary motion of the first kind becomes predominant.

In contrast to Prandtl's second kind of secondary flow, which is present in turbulent non-circular duct flows, are often described as "turbulence-driven secondary flow". Although such motion is two order of magnitude smaller than the mean flow velocity it may have important consequence. For example, it causes the contours of main velocity to bulge towards the corners and produces an overall increase in the boundary sheer stress. Effects such as these are important in many flows of industrial interest. Examples are flows in turbomachinery, heat exchangers, nuclear reactors, ventilation and air conditioning systems and open channels. All such flows are companied by turbulence driven secondary flow motions in the plane perpendicular to the main flow direction. One of these applications, namely the flows in turbomachinery, the flow is more complex due to the interaction of turbulence field with body forces arising from rotation of duct. Body forces act both directly on the mean flow motion and on the turbulence fluctuations.

The flow in the above mentioned situation is too complicated to investigate experimentally at a reasonable expense. Complex equipment's are needed to perform the experiments which can be very time consuming. The alternative is to try to develop a numerical model to simulate the flow. The present study describes the application of a finite difference solution procedures to the differential equations that govern the flow. The study is restricted to steady, fully developed, flow of an incompressible Newtonian fluid. Calculations have been made for stationary ducts, while recommend to make the calculations based on rotating ducts as well. Furthermore, the study covers ducts with one-to-one aspect ratio (square duct). In all conditions the predicted results obtained from this work have been compared with available experimental and computational data.

1.2 Calculation Method of Turbulence Flows:

It is generally accepted that Navier-Stokes equations together with the continuity equation comprise a closed set of equations the solution of which provides a valid description of any laminar or turbulent flow. The continuity equation for a constant density steady flow can be written as:

$$\frac{\partial \widehat{U}_i}{\partial x_i} = 0 \qquad 1.1$$

Where $\widehat{U}_i$ is the instantaneous velocity in the x_i direction. The Navier-Stokes equations for the steady flow of a Newtonian fluid of viscosity μ and in the absence of body forces take the form:

$$\rho \frac{\partial \widehat{U}_i \widehat{U}_j}{\partial x_j} = -\frac{\partial \hat{P}}{\partial x_i} + \frac{\partial \hat{\tau}_{ij}}{\partial x_j} \qquad 1.2$$

For ease of calculations, the statistical average of $\widehat{U}$ and $\hat{P}$ with respect to time can be written as the following:

$$U_i = \lim_{t\to\infty} \int_t^{t+\Delta t} \widehat{U}_i \, dt \qquad 1.3a$$

$$P = \lim_{t\to\infty} \int_t^{t+\Delta t} \hat{P} \, dt \qquad 1.3b$$

Where U & P are the average values of $\widehat{U}$ and $\hat{P}$ and Δt represents a time interval greater than the time of slowest fluctuations. The random fluctuations in U and P (u and p) are defined as:

$$u_i = \widehat{U}_i - U_i \qquad 1.4a$$

$$p = \hat{P} - P \qquad 1.4b$$

Substitution for $\widehat{U}$ and $\hat{P}$ in equations 1.1 and 1.2 with the relation 1.4 and time averaging yields:

$$\frac{\partial U_i}{\partial x_i} = 0 \qquad 1.5$$

$$\rho \frac{\partial U_i U_j}{\partial x_j} = -\frac{\partial P}{\partial x_i} + \frac{\partial \tau_{ij}}{\partial x_j} + \frac{\partial\left(-\rho \overline{u_i u_j}\right)}{\partial x_j} \quad 1.6$$

Because equation 1.2 is nonlinear the averaging process has led to the appearance of unknowned second order correlations $\left(-\rho \overline{u_i u_j}\right)$ in equation 1.6. These correlations represent the transport of momentum due to the turbulent motion and are known as "Reynolds stress". The appearance of these extra unkowns results in a non closed system of equations. In fact, the determination of Reynolds stress is the main problem in claculating turbulent flows. Althogh exact transport equations can be derived for the Reynolds stress, these equations contain turbulent correlations of the next higher order. This is known as the "closure problem". Therfore, closure of the equations cannot be obtained by restoring to equations for correlations of higher and higher order. Instead, a turbulence model must be introduced.

In broad terms, the turbulence model is used to approximate the Reynolds stress in terms of known quantities. In sophisticated models, the Reynolds stress are obtained from the solution of modelled diffrential equations which describs the rate of tranport, generation and destuction of each component of stress tensor. These models are often reffered to as "second-order closuer models". Examples of such schemes include the Reynolds stress model (RSM) and algebra stress model (ASM).

1.3 Objectives of the Present Study:

The present study is primarily motivated by the need for a generally practical prediction procedure for turbulent flow in ducts of non-circular cross-sections. From the points considered in the previous section it is clear that the second-order closure models seem to be limited in use in practical engineering.

An alternative approach of practical aspect has been treated in order to allow the RSM turbulence model to predict the turbulence driven secondary flow motions. The purpose of the present work is to add to knowledge in this field. However, the main objectives of present study are as follows:

1) To investigate the capability of K-ϵ, RSM & LES models, whether correctly predict the turbulence-driven secondary motion in straight non-circular ducts.
2) To predict using RSM model the distribution of boundary shear stress and turbulence structure for fully developed flows in a square duct.

1.4 Outline of the thesis:

The rest chapters of present thesis are arranged as follows:

- In chapter 2, a brief review is made of previous excremental and theatrical investigations of turbulent flow in non-circular ducts.
- In chapter 3, the partial differential equations which govern the flow considered here are derived. These equations are then transformed into their finite difference equivalents and the method used for their solution is presented.
- In chapter 4, the turbulence model is discussed and the mathematical details of present RSM turbulence model.
- In chapter 5, detailed discussions on the results obtained for the turbulence-driven secondary motion in stationary non-circular square ducts. The chapter also illustrates the comparisons with other experimental work.
- In chapter 6, a summary of the main achievements of the present study and recommendations for future research.

CHAPTER FIVE

Results & Discussions

5.1 Introduction:

In the present chapter, the validation of solving the flow in by using Reynolds Stress Model (RSM), as a Comparisons between the turbulence models (RSM) and the experimental work of Melling and Whitelaw (1976) are presented for a Reynolds number of Re = 42000.

Calculations for fully turbulent flow have been performed for square duct (B/H=1). The emphasis throughout has been on the prediction area for which detailed experimental as described in this chapter, for the sake of comparison.

This chapter comprises three main sections. Information on the duct description and grid used for numerical simulation by the turbulence model (RSM) are given in section 5.2. Details for the used flowing fluid are provided per section 5.3. However, detailed boundary conditions have been illustrated per section 5.4. The major parts of the study deal with the comparison between the experimental work of Melling Whitelaw (1976) and computational fluid dynamics results considering turbulence model (RSM), all results for main flow as well as the turbulence structures are presented and discussed in section 5.5. Finally, a brief summary of the achievement of this chapter is contained in section 5.6.

5.2 Duct and grid description:

The flow domain of interest in the present computational study is illustrated in Figure 5.1 , the figure presents square horizontal duct, with cross-sectional area of (30 cm x 30 cm), and length of (450 cm). Also, the figure represents the x-y cross-sectional plane of the duct, the main flow direction being normal to this plane (in the z direction).

The grids used by the wall function (30x30) are shown in Figure 2. with “enhanced wall treatment is used for the near-wall treatment”. This is ascertaining that, turbulence quantities in turbulent flows are properly resolved with high accuracy.

Hence, for the current study, sufficiently fine meshes are used near to duct wall and duct corners with more cells & nodes are generated in duct corners where the secondary flow is predicted, so that more accurate results can be generated beside the corners.

Grid size/details for the studied case are:

- Total Number of Cells: 1,265,625
- Total Number of Faces: 3,819,375
- Total Number of Nodes: 1,305,376

Furthermore, Owing to the symmetry of the ducts about its two center planes in stationary flow conditions, and to obtain more accurate results, the study have been emphasized on one quarter of the duct only (the top-right quarter), with considering "Periodic Boundaries" that allows to generate more nodes and finer mish for fluid domain, while the results for complete geometry can be viewed by mirroring or repeating the domain. The boundaries of the calculation domain in such a case are mathematically defined as follows: the top & right boundaries are the stationary half walls of the ducts at which all the velocities are zero, while the bottom & left boundaries are the symmetry planes across which the flux of any variable is zero.

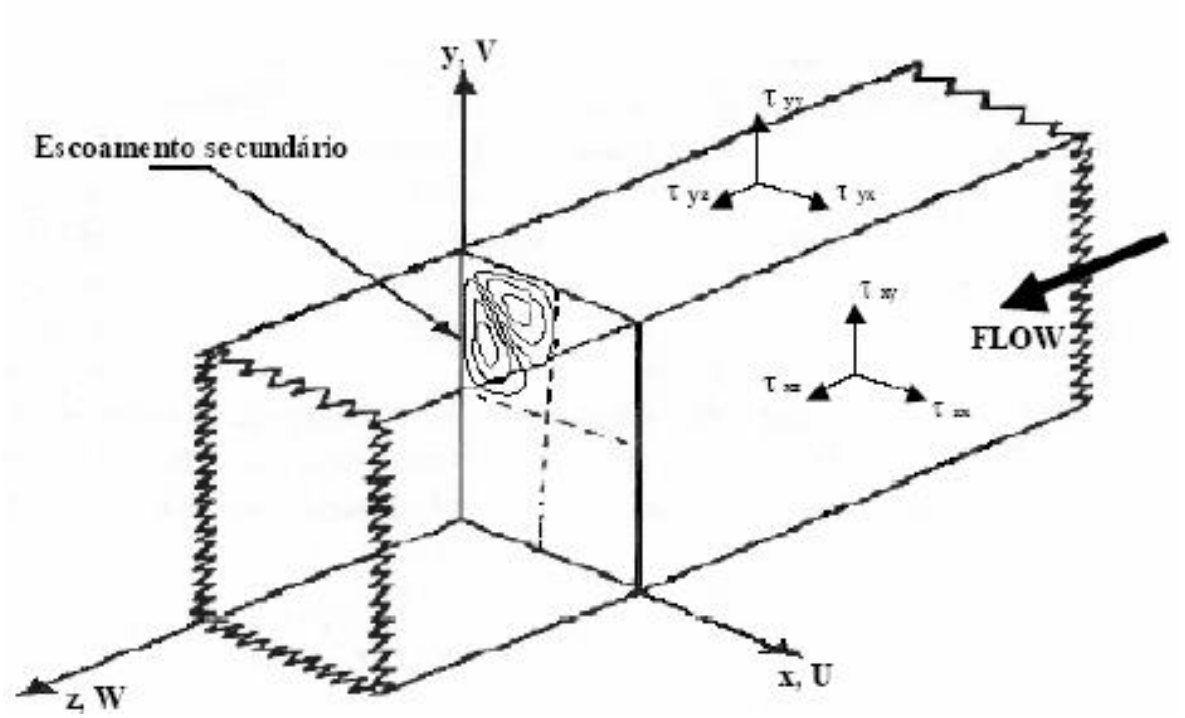

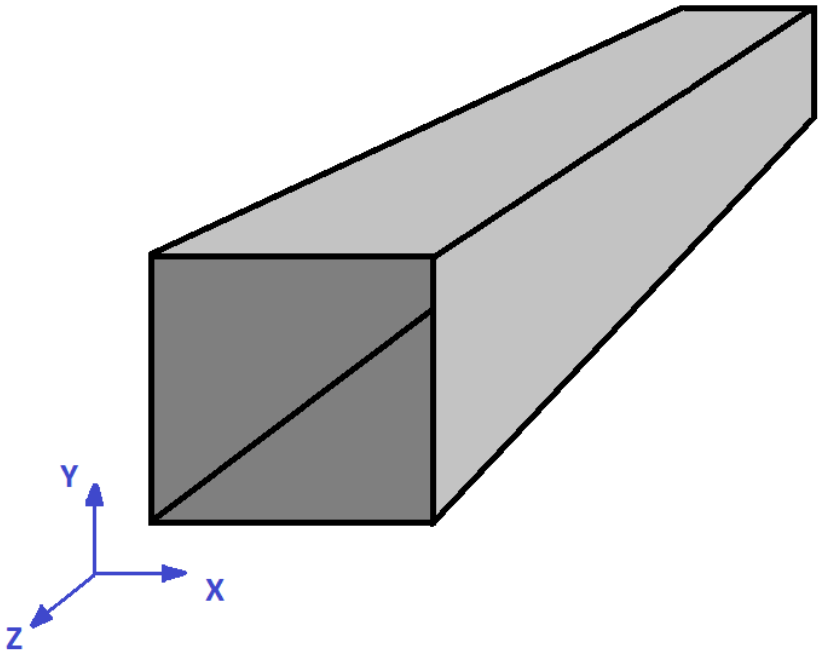

FIG. (5.1): DUCT 30 x 30 x 450 cm

The secondary flow streamlines are also shown in (Figure 5.2). The flow direction occurs from the center to the corners and returns to the center along the walls, forming eight vortexes. It is noticed that Melling and Whitelaw (1976) don't show the secondary flow streamlines, only a vectors distribution of secondary velocity, without symmetry, making comparisons difficult. The models predict streamlines very similar.

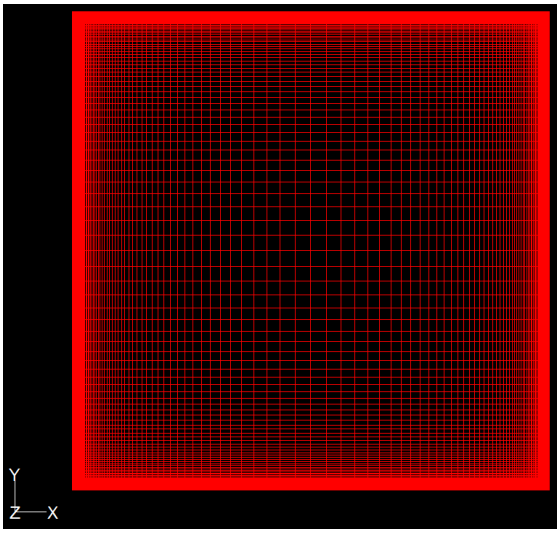

FIG. (5.2): GRID

5.3 Flowing fluid:

To simplify the current study, “Air” is considered as the flowing fluid through the duct. Also, standard physical properties are considered for the current study, these standard physical conditions are provided per FLUENT data base, below (figure 5.3) shows these physical properties.

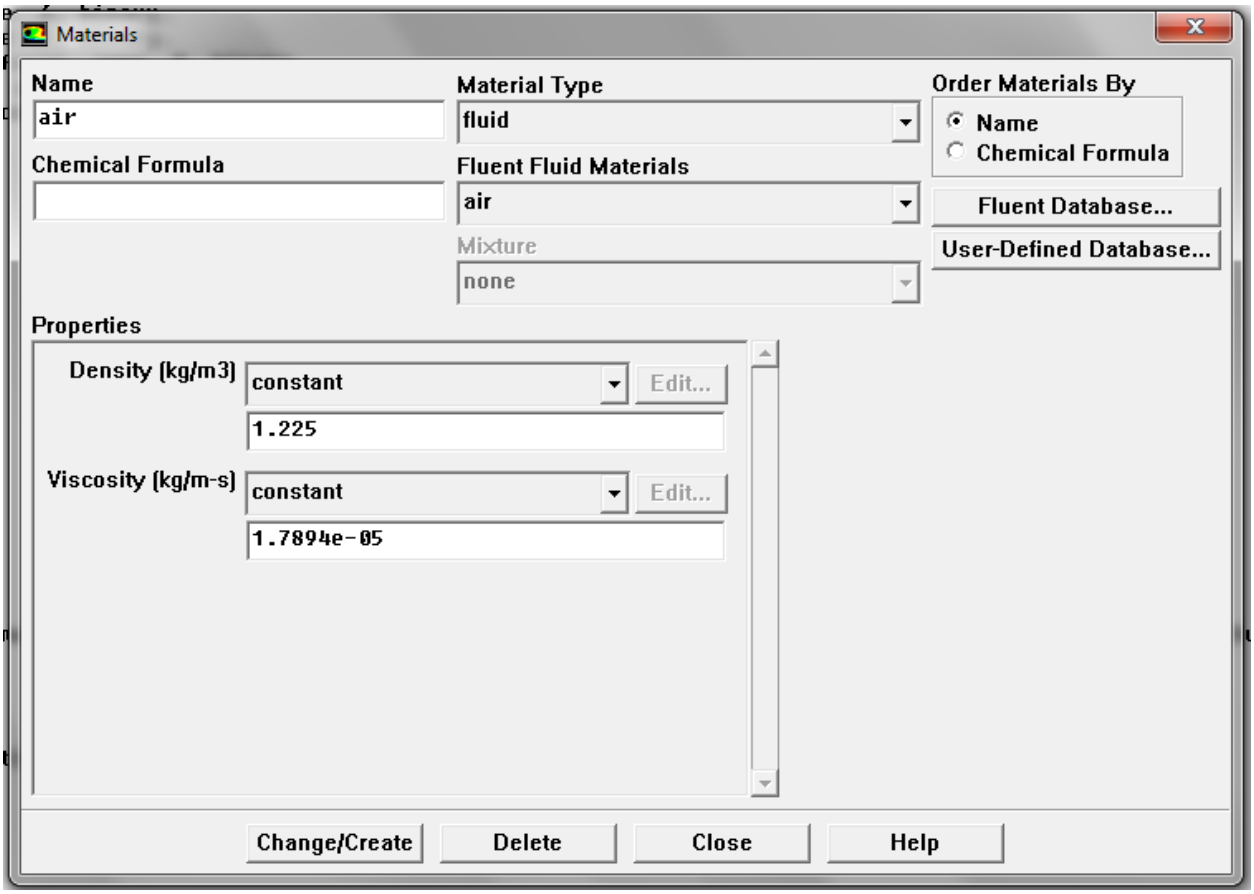

FIG. (5.3): Air physical properties

5.4 Boundary conditions:

Boundary conditions specify the flow and thermal variables on the boundaries of the physical model subjected to the study. They are, therefore, a critical component of FLUENT simulations study cases.

As illustrated in section 5.2, two types of boundary conditions (i.e. constrains on the dependent variables at the four boundaries of cross-sectional planes of all value of z axis) are encountered in the present thesis: stationary duct walls and planes of symmetry. Initially, all component of velocity are zero. For the near-wall region, special practices (such as enhanced wall treatment) are needed for the reasons discussed below. In central region of the flow, the gradient of flow properties is usually not very steep; a moderately fine grid yields reasonable accurate solutions. Close to the walls, the variable gradients become much steeper, thus an extremely fine grid is necessary for their accurate computation.

The boundary types available in FLUENT are classified as follows:

- Flow inlet and exit boundaries: pressure inlet, velocity inlet, mass flow inlet, inlet vent, intake fan, pressure outlet, outlet flow, outlet vent, and exhaust fan.
- Wall, repeating, and pole boundaries: wall, symmetry, periodic, axis
- Internal cell zones: fluid, solid (porous is a type of fluid zone)
- Internal face boundaries: fan, radiator, porous jump, wall, interior and it is important that they are specified appropriately

Here under a detailed illustration for all boundaries conditions have been considered for computation by using turbulence model (RSM):

5.4.1 Inlet Boundary Conditions:

Inlet Velocity boundary condition is the main boundary conditions used for the present study, Velocity magnitude is 7 m/sec in direction of z-axis normal to the boundary. Also, turbulence specifications used are shown in below screen shot (figure 5.4), with turbulence intensity (2%) and hydraulic diameter of (0.3m). More importantly, all computations for flowing fluid properties by turbulence model (RSM) have be initiated from inlet velocity boundary conditions.

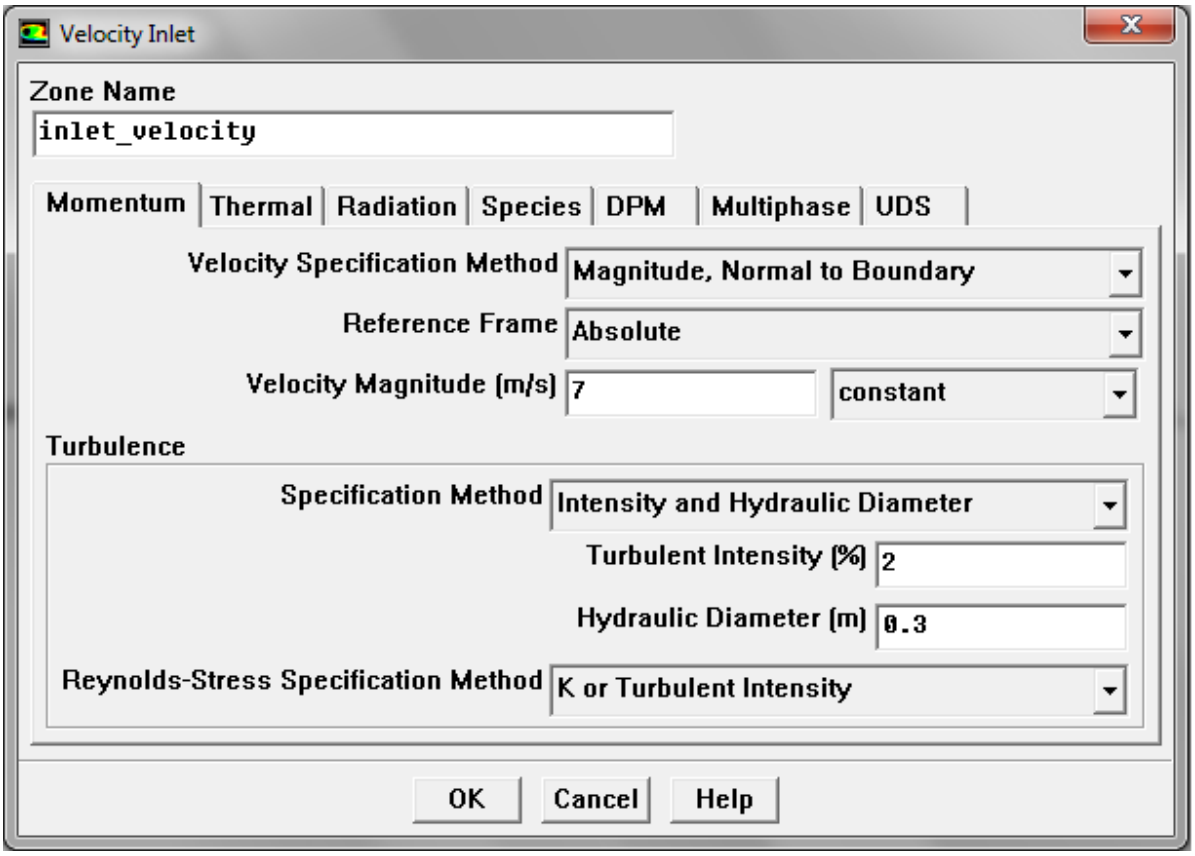

FIG. (5.4): Inlet boundary conditions

5.4.2 Outlet Boundary Conditions:

For outlet boundary conditions, we have considered atmospheric pressure at duct outlet. Below screen shot (figure 5.5) reflects all considerations for this boundary condition.

FIG. (5.5): Outlet boundary conditions

5.4.3 Walls Boundary Conditions:

As illustrated earlier, due to planes of symmetry we have considered wall boundary conditions for the top & right edges. Below screen shot (figure 5.6) reflects all consideration for Wall roughness, Wall motion (stationary), and shear conditions (no slip).

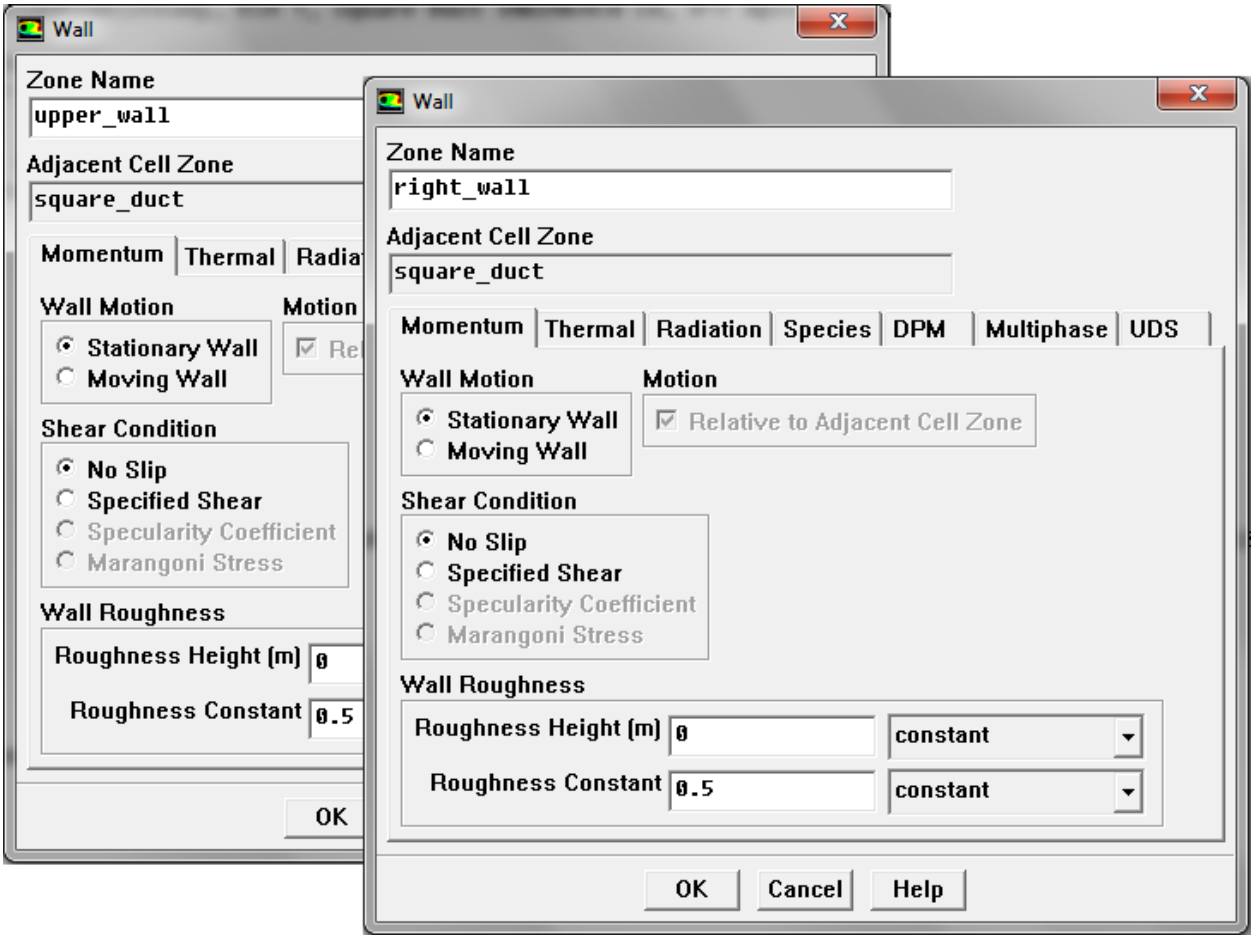

FIG. (5.6): Walls boundary conditions

5.4.4 Periodic Boundary Conditions:

As illustrated earlier, the bottom & left boundaries are periodic boundary conditions; hence we have considered Periodic boundary conditions for the bottom & left edges. Also, for displayed results, we have viewed the results for complete duct by repeating the studied domain (duct quarter) four times by rotating it with 90 Degrees about the z axis as shown in (figure 5.7).

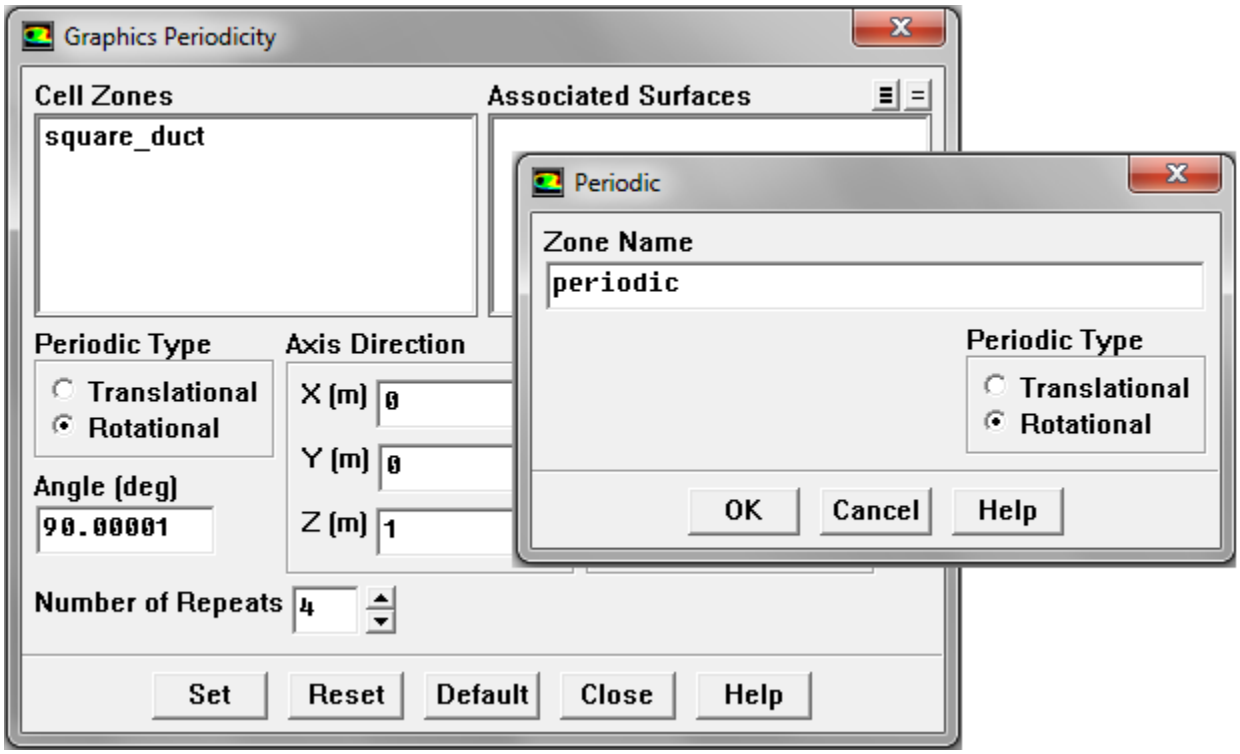

FIG. (5.7): Periodic boundary conditions

5.5 Results:

5.5.1 Main Axial Velocity:

Mean axial velocities along the duct center-line are presented in figures 5.8 by considering three inlet velocities (V= 2 m/s, V= 7 m/s and V= 14 m/s) by using turbulence modeling RSM. These figures show the axial velocity and turbulent kinetic energy fields, respectively, it was adimensionalized utilizing the maximum axial velocity value. It can be noticed that, due to the fact that the secondary flow is associated with the turbulence, the field of axial velocity is distorted. Due to the symmetry of the flow, the results are shown only for a quadrant of the square duct.

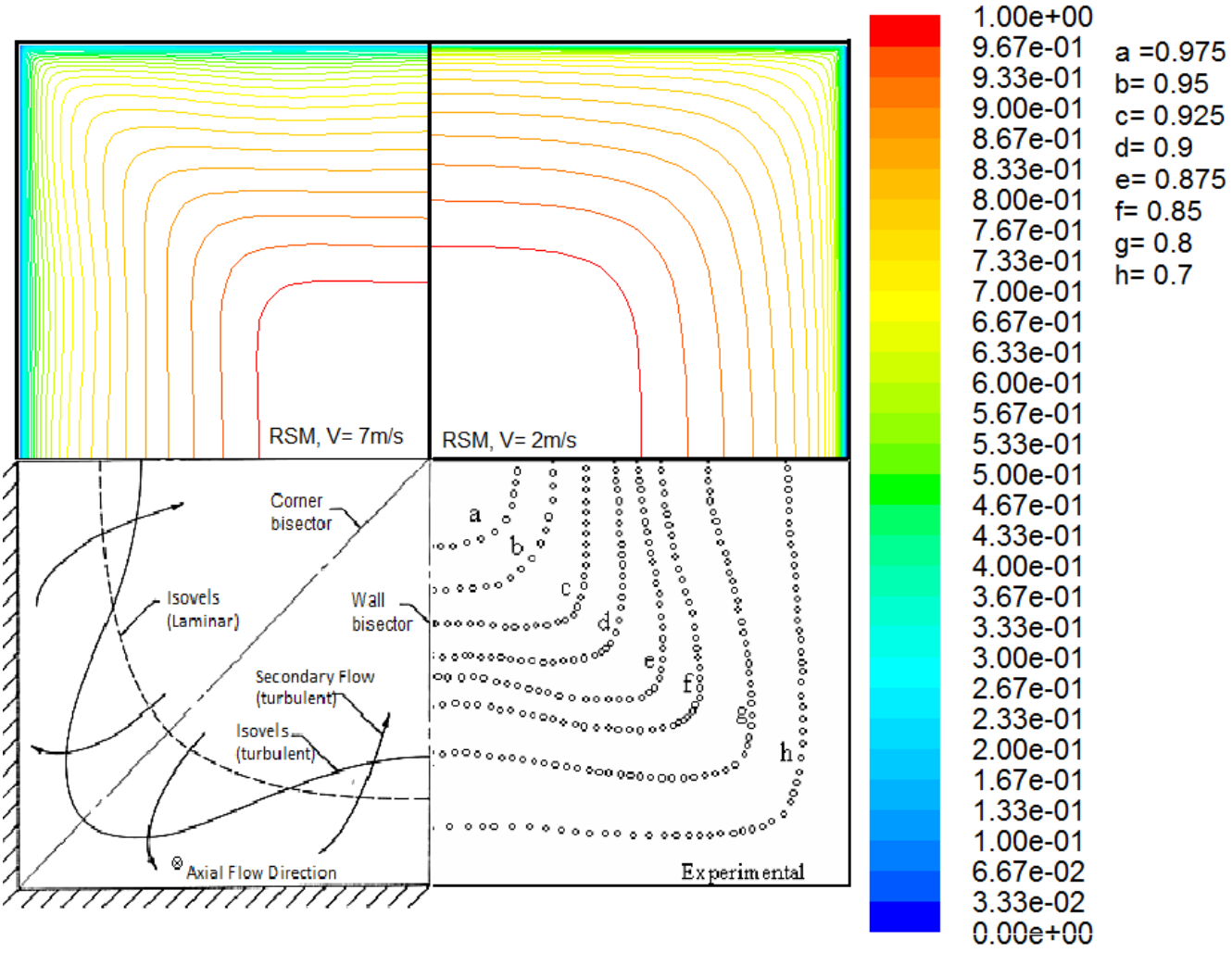

FIG. (5.8): Axial mean velocity contours W /W_{max} , Experimental by Melling and Whitelaw [7]

The isovels plots obtained with present turbulence model RSM have been compared with the experimental data work of Melling and Whitelaw (1976), where eight contours of the primary velocities normalized with the maximum velocity (W /W_{max} = 0.7, 0.8, 0.85, 0.875, 0.9, 0.925, 0.95, and 0.875) are plotted. All models show little bulging of the contours towards the corners in comparison with the data measured by Melling and Whitelaw (1976). In survey on the development of turbulent flow in non-circular ducts, Kline (1981) found that the length required for full flow development may exceed 140 pip diameters and for certain inlet conditions, it was advised to be as low as 70 D_h. However, no definite conclusion can be proved. In view of the uncertainties about the fully developed conditions, the present model can be considered in fair agreement with experimental contours.

As a result from figure 5.7 the mean velocity contours are bulging due the action of the secondary flow which acts to transport high momentum fluid away from the core. However, the reason for the difference between present model and experimental data lies in the predicted secondary motion as will be shown in the next section.

5.5.2 Secondary flow streamlines:

Secondary flow streamlines at outlet flow cross-sectional area of the duct are presented in figures 5.9, the secondary flow velocity vectors are observed to be directed along each wall bisector towards the core region, and then deflected along with the diagonals towards the corners, forming eight shape vortexes.

It is noticed that Melling and Whitelaw (1976) don't show the secondary flow streamlines, only a vectors distribution of secondary velocity, without symmetry, making comparisons difficult. The models predict streamlines very similar. Furthermore, below secondary flow streamlines have been colored by velocity magnitude, however, the maximum values of velocities in x and y directions, which occur on the diagonals near the corner, do not exceed 0.162 m/s taking into consideration that the maximum axial velocity at z direction velocity is 8.82 m/s. Hence, the max velocity of secondary flow does not exceed 2% of main axial velocity.

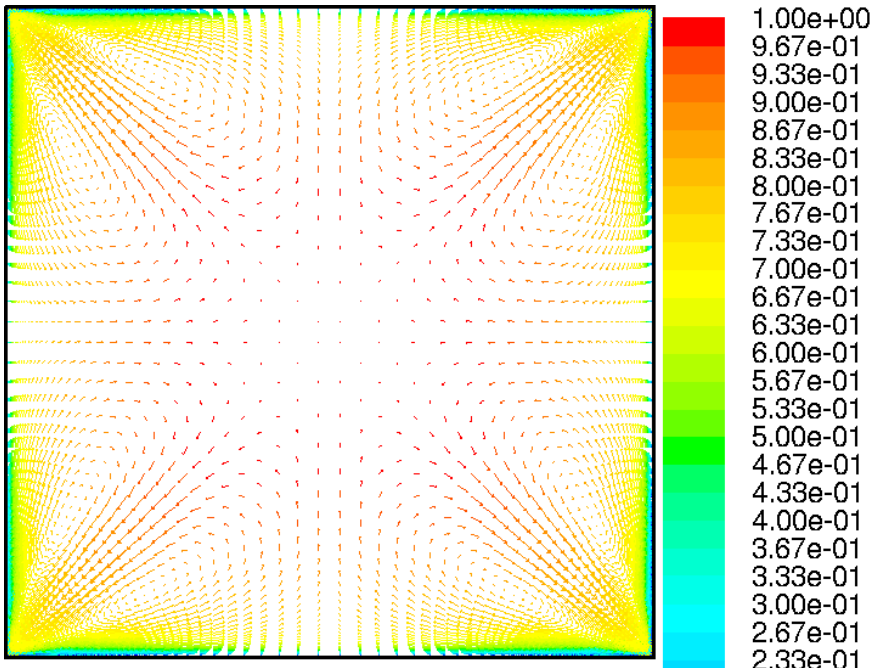

Secondary flow streamlines for RSM (V= 2m/s)

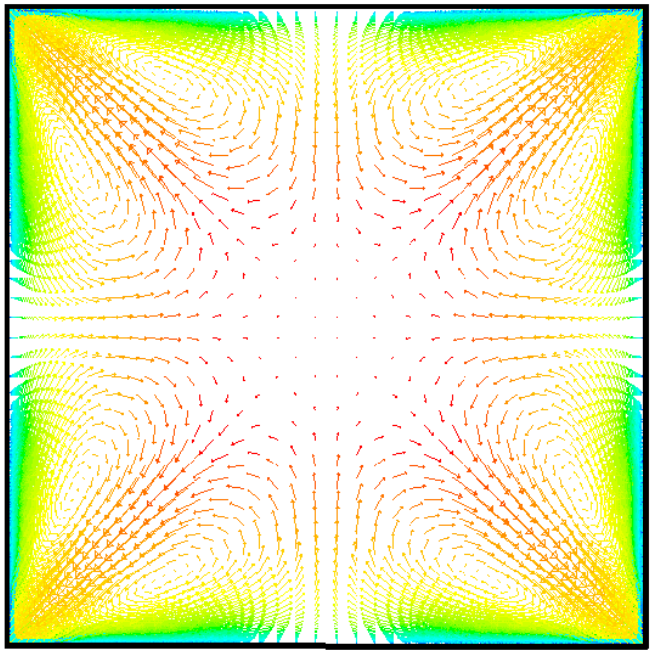

Secondary flow streamlines for RSM (V= 7m/s)

FIG. (5.9): Secondary Flow Streamlines – using (RSM)

The predicted distributions secondary velocity streamlines (normalized by D_h and the centerline velocity) in a square duct are compared for two values of inlet velocities, the first is

V= 2m/s and the second is V= 7m/s. the secondary flow streamlines are obviously reflected for V= 7 m/s.

Furthermore, for both figures, a pair of longitudinal vortices is produced, one vortex over the corner bisector is called “side vortex”, and the other vortex under the bisector is called “bottom-vortex”. In the square duct condition, as it is expected, the side-vortex and the bottom vortex are well symmetrical with each other in regard to bisector. The pattern of the bottom-vortex is completely confined by the side wall and thus the effect of change in the duct aspect ratio small. On the other hand, the side-vortex is much affected by the aspect ratio: increase in the aspect ratio leads to a decrease in side-vortex and then tends to attain a constant at high aspect ratio. This bisector is well predicted by the present model.

5.5.3 Turbulence Kinetic Energy:

Turbulence kinetic energy which can be considered as the scale of the turbulence intensity in the three dimensional flow investigated in the present thesis is plotted in figure 5.9 normalized by the max velocity W_{max}. It can be noticed that, due to the fact that the secondary flow is associated with the turbulence, the field of axial velocity is distorted. Due to the symmetry of the flow, the results are shown only for a quadrant of the square duct. The model that presents smallest deviations from the experimental data is the RSM, with inlet velocity v= 7 m/s.

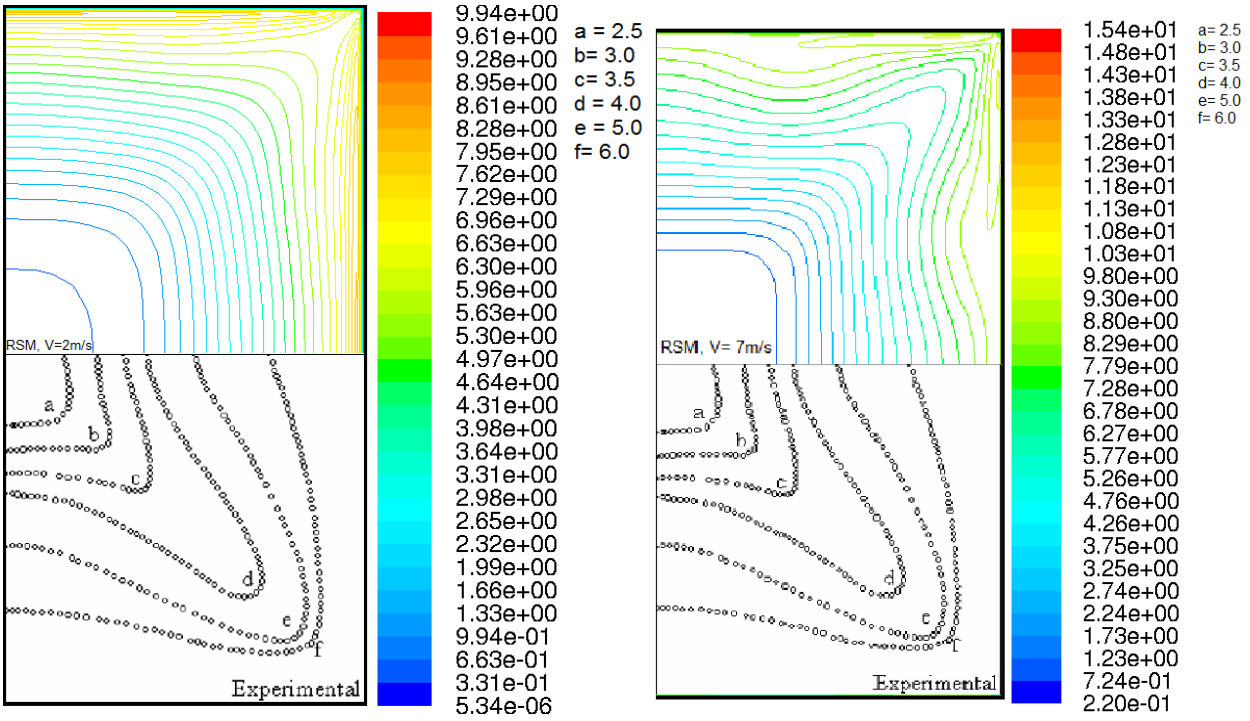

FIG. (5.10): Turbulent kinetic energy contours, $k\ /(W_{max})^2 * \ 1000$, Experimental by Melling and Whitelaw [7]

5.5.4 Turbulent intensity contours:

Predicted turbulence quantities are displayed in figures 5.10, 5.11, and 5.12 for the square ducts, considering different inlet velocities (V= 2 m/s & V= 7 m/s). The results clearly show the capability of Turbulence model to correctly predict the shear stress distributions. The contour map of Reynolds normal stress in the x-direction τ_{xx} (sometimes referred as transverse turbulence intensity) shown in this figure.

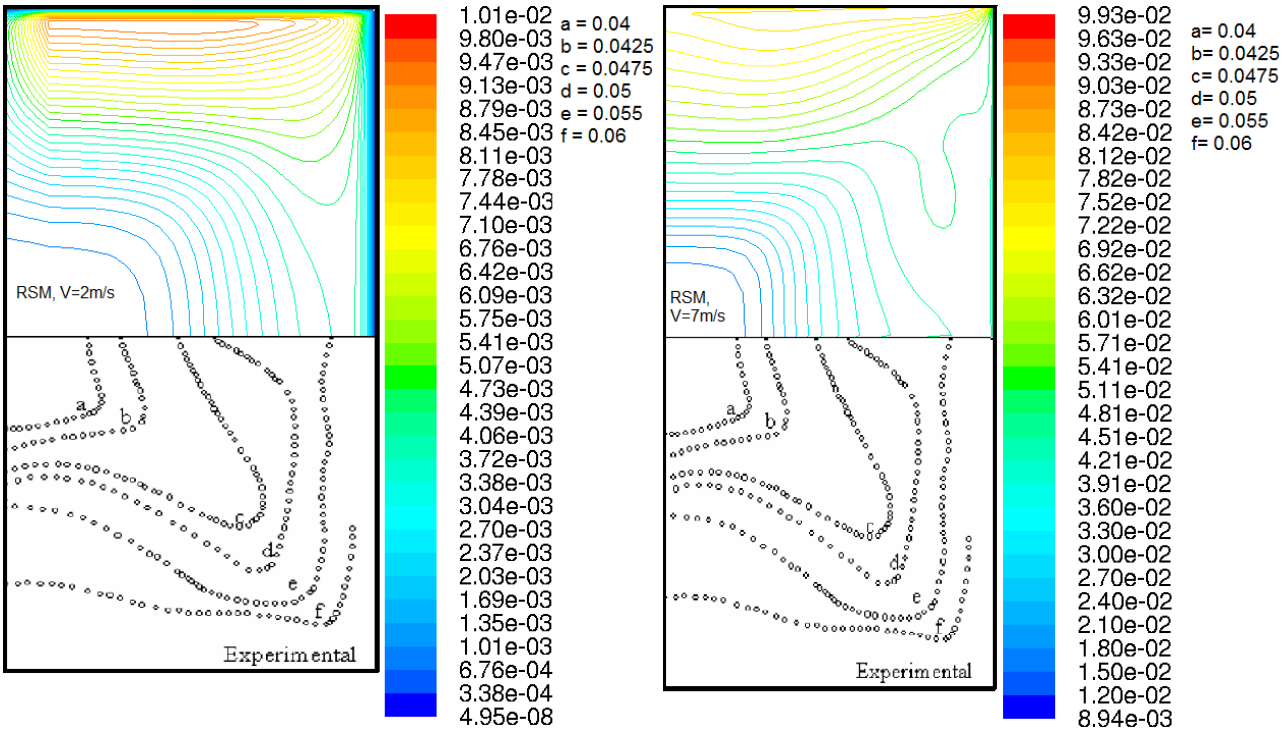

FIG. (5.11) : Turbulent intensity contours $\acute{u}/W_{max}$, Experimental by Melling and Whitelaw [7]

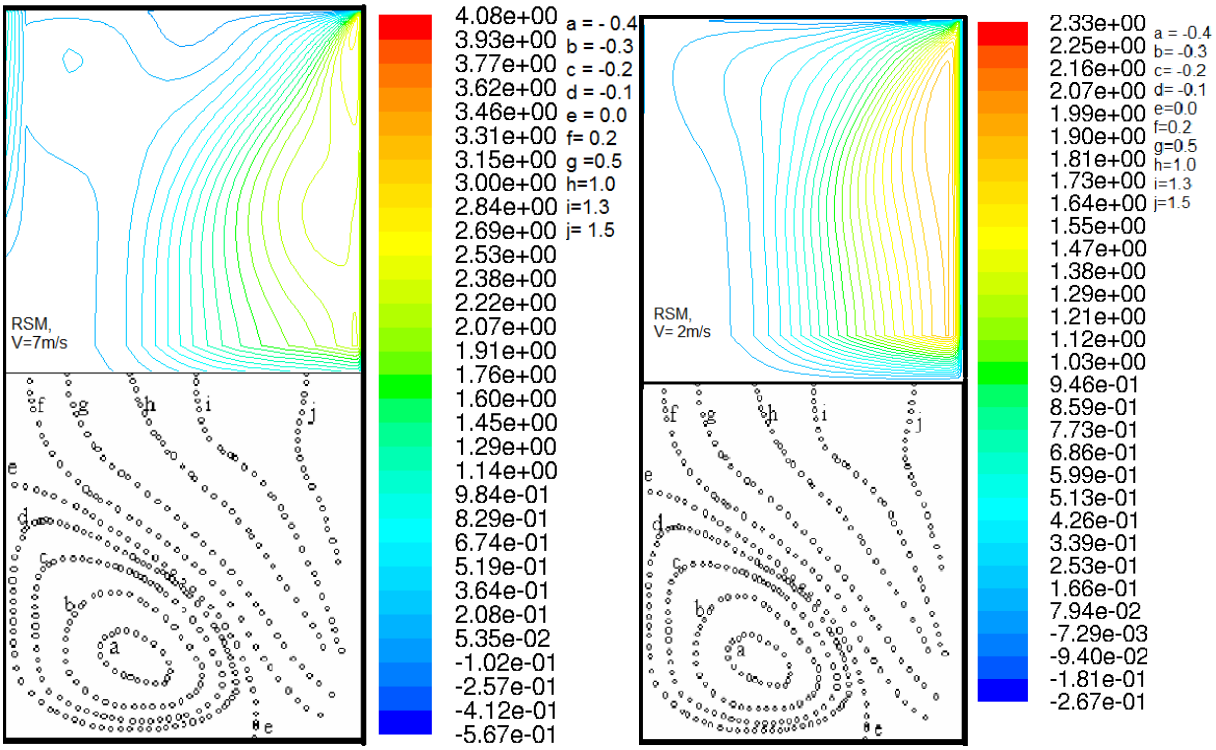

FIG. (5.12) : Turbulent intensity contours $\acute{u}\acute{w}/(W_{max})^2 * 1000$, Experimental by Melling and Whitelaw [7]

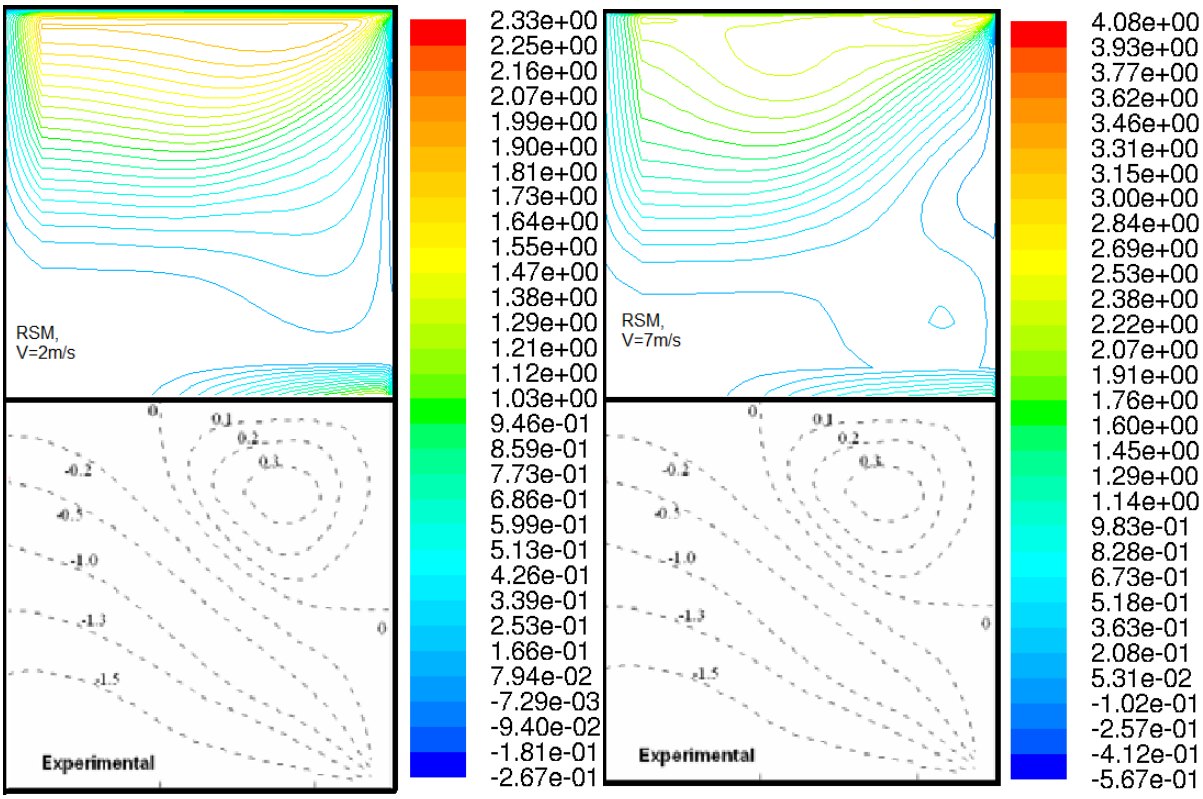

FIG. (5.13): Turbulent intensity contours $\acute{v}\acute{w}/(W_{max})^2 * 1000$, Experimental by Melling and Whitelaw [7]

5.6 Closure:

In this chapter, the results of calculations performed with the turbulence model RSM. The emphasis has been placed on the prediction of the turbulent flow situations investigated by experimental work. Hence, fully developed square duct has received the greatest attention. The numerical procedure, incorporating the present turbulence model has been applied successfully to the prediction of turbulence driven secondary motion in three dimensional flows. The capability of RSM turbulence model to correctly predict each motion has been confirmed. The secondary flow pattern has been predicted well, although its magnitude close to the wall are slightly overestimated in comparison with the experimental data.

The computed distributions of the mean axial velocity, turbulence energy and wall sheer stress found to be in very favorable agreement with the available experimental data.

However, the present results of RSM turbulence model represent a very appreciable improvement on the other turbulence models hitherto performed.

CHAPTER SIX

Conclusion

The final chapter in this thesis is in two sections. The extent to which the objective s of this work, as outlined in section 1.3, have or have not been fulfilled is discussed in section 6.1. Suggestions for further work are presented in section 6.2

6.1 Achievement of Objectives:

The first of the present objective was to investigate the capability of RSM turbulence model of predicting turbulence-driven secondary flows. The flow patterns are drawn in GAMBIT, specifying all boundaries conditions, and then establish the mesh for the flow pattern, with applying fine grid near to the wall, where secondary flow is predicted.

The K-ϵ, LES, and RSM turbulence models were then applied to predict the fully-developed flow in a square duct at various Reynolds numbers. It was clear that only RSM turbulence model is capable of reproducing the turbulence anisotropy required to drive the secondary motion. The first objective was thus attained and the second objective, concerned with a detailed study of the mean-flow and turbulence structure in a square duct, was tackled next. Published experimental data for fully-developed flows in square ducts were used to test RSM turbulence model performance over two values of Reynolds numbers. Comparison were also made with experimental work carried out by Melling and Whitelaw (1976) that consider a Reynolds number of Re = 42000.

Overall, the RSM turbulence model produced results that are similar and in many cases better than other turbulence models such as The K-ϵ and LES turbulence models. In particular, the expected distortion in main-velocity contours due to the secondary flow was well reproduced, and so was the shift in the location of wall shear stress away from the center planes and towards the corners. The turbulence model (RSM) also produced close agreement with turbulence data including the imbalance in normal stress generating the secondary flow. Hence, Objective two has clearly been attained.

6.2 Recommendation for Future Work:

This study has focused on flows in square ducts because those are better documented experimentally. However, several other cross-sections may be encountered in practice (such as rectangular with wide range of aspect ratios, triangular, and curved triangular that occur in rod bundles) where the effects of turbulence-driven flow are equally important. It is therefore recommended that the present study to be extended to such complex geometries. Specially, to apply the same turbulence model (RSM) for rectangular ducts with different aspect ratios in order to obtain a better indication of the effect of duct aspect ratio on the distribution of turbulence-driven secondary flow.

Further extension should include the prediction of heat transfer in non-circular ducts with aid of the present turbulence model.

Finally, it is recommended to complete the present study and use the turbulence model (RSM) to predict the secondary motion in a non-circular rotating ducts of varying aspect ratios.

REFRENCES

[1] Hoagland, L. C. "Fully Developed Turbulent Flow In Straight Rectangular Ducts – Secondary Flow, Its Cause and Effect on The Primary Flow", Massachusetts of Technology, September 1960.

[2] Güleren, K. M. "Large-Eddy Simulation Of Wall-Bounded Flows Subjected To Curvature And Rotation", School of Mechanical, Aerospace and Civil Engineering, May, 2007.

[3] Uruba, V. and Hladík, O. and Jonáš P. "Dynamics Of Secondary Flow In Rectangular Channel", Institute of Thermomechanics AS CR, v.v.i., Prague, October 2011.

[4] FLUENT, "FLUENT 6.2 User's Guide", Fluent Inc, Lebanon, 2005.

[5] Rivas, G. A. and Garcia, E. C. and Assato, M. "Turbulent Flow Simulations In A Square-Duct Using Non-Linear And Reynolds Stress Models", Instituto Tecnológico de Aeronáutica & Pontifícia Universidade Católica, Brazil, 2008.

[6] Abdellatif, O. E. "Numerical Simulation Of Turbulence-Driven Secondary Flows In Non-Circular Ducts With And Without Rotation", Shoubra Faculty Of Engineering, Zagazig University, Egypt, 1990.

[7] Melling, A. and Whitelaw, "Turbulent Flow In A Rectangular Duct ", J. Fluid Mech., J.H., 1976.

[8] Zhang, J. and Li, A. "Study On Particle Deposition In Vertical Square Ventilation Duct Flows By Different Models", School of Environmental and Municipal Engineering, China, October 2007.

[9] ICASE "Reports On Numerical Study Of Turbulent Secondary Flows In Curved Ducts", NASA Virginia, 1989.

[10] ICASE "Reports On The Prediction Of Turbulent Secondary Flows", NASA Virginia, 1992.

[11] Habip Asan, E.S.M.E and M.S.M.E "A Computational Study Of Laminar And Turbulent Flows In Rotating Rectangular Ducts", Texas, 1993.

[12] Huser, A. and Bringen, S. "Direct Numerical Simulation Of Turbulent Flow In A Square Duct", Department of Aerospace Engineering Sciences, University of Colorado, Boulder ،CO 80309, USA, 1993.

[13] Huser, A. and Biringen, S. and Hatay, F. F. "Direct simulation of turbulent flow in a square duct Reynolds-stress budgets", University of Colorado at Boulder, Boulder, Colorado 80309, 1994.

[14] Madhav, M. T. and Malin, M. R. "The Numerical Simulation Of Fully Developed Duct Flows", CHAM Limited, Wimbledon, London, UK, 1997.

[15] Pallares, J. and Davidson, L. "Large-Eddy Simulations Of Turbulent Flows In Stationary And Rotating Channels And In A Stationary Square Duct", Chalmers University Of Technology, 2000.

[16] Nordsveen, M. "Wave- And Turbulence-Induced Secondary Currents In The Liquid Phase In Stratified Duct Flow", Studsvik Scandpower, Norway, 2001.

[17] M°artensson, G. E. and Brethouwer, G. and Johansson, A. V. "Direct Numerical Simulation Of Rotating Turbulent Duct Flow", Royal Institute of Technology (KTH), Sweden, 2004.

[18] Winkler, C. M. and Rani, S. L. and Vanka, S. P. "A Numerical Study Of Particle Wall-Deposition In A Turbulent Square Duct Flow", Boeing Company, CFD Research Corporation, University of Illinois at Urbana-Champaign, Urbana, IL 61801, USA , 2005.

[19] Chiu, H. C. and Jang, J. H. and Yan, W. M. "Combined Mixed Convection And Radiation Heat Transfer In Rectangular Ducts Rotating About A Parallel Axis", Technology and Science Institute of Northern Taiwan and Huafan University, Shih Ting, Taipei 223, Taiwan, 2006.

[20] Hashemabadi, S. H. and Etemad, S. Gh. "Effect Of Rounded Corners On The Secondary Flow Of Viscoelastic Fluids Through Non-Circular Ducts", Iran University of Science and Technology, and Isfahan University of Technology, Iran, 2005.

[21] Ma, L. D. and Li Z. Y. and Tao W. Q. "Direct Numerical Simulation Of Turbulent Flow And Heat Transfer In A Square Duct With Natural Convection", School of Energy and Power Engineering ‹Xi' an Jiaotong University, Xi'an, China, 2007.

[22] Arts, T. and Benocci, C. and Rambaud, P. "Experimental And Numerical Investigation Of Flow And Heat Transfer In A Ribbed Square Duct", Von Karman Institute for Fluid Dynamics, B-1640 Rhode-Saint-Genèse, Belgium, 2007.

[23] Uhlmann, M. and Li, A. P. and Kawahara, G. and Sekimoto, A. "Marginally Turbulent Flow In A Square Duct", Modeling and Numerical Simulation Unit, CIEMAT, 28040 Madrid, Spain and Department of Mechanical Science, Osaka University, 560-8531 Osaka, Japan, 2007.

[24] Pecnik, R. and Iaccarino, G. "Predictions Of Turbulent Secondary Flows Using The $v^2 - f$ Model", Center for Turbulence Research, 2007.

[25] Pattison, M. J. and Premnath, K. N. and Banerjee, S. "Turbulence-Induced Secondary Flows In A Square Duct Using A Multiple-Relaxation-Time Lattice-Boltzmann Approach", Meta Heuristics LLC, Santa Barbara, CA 93105 and Department of Chemical Engineering, University of California, USA, 2007.

[26] Pattison, M. J. and Premnath, K. N. and Banerjee, S. "Computation Of Turbulent Flow And Secondary Motions In A Square Duct Using A Forced Generalized Lattice-Boltzmann Equation", Meta Heuristics LLC, Department of Chemical Engineering ،University of California, Bren School of Environmental Science and Management University of California ،Santa Barbara, 2008.

[27] Soualmia A. and Zaouali, S. and Labiod, C. "Modeling Of Secondary Motions Driven By The Turbulence Anisotropy In Closed And Open Channels", Ecole Nationale d'Ingénieurs de Tunis, LMHE, B.P. 37 Le Belvédère, 1002 Tunis, Tunisie & Université de Jijel, Laboratoire de Génie Géologique, B.P. 98, Ouled Aissa, 18000 Jijel ،Algérie, 1991.

[28] Akcayoglu, A. and Sahin, B. and Canpolat, C. and Akilli, H. "Experimental Flow Results In A Non-Circular Duct With Heat Transfer Augmenting Obstacles", Proceedings of the World Congress on Engineering 2010 Vol II WCE 2010, June 30 - July 2, 2010, London, U.K., 2010.

[29] Zhu, Z. and Yang, H. and Chen, T. "Numerical Study Of Turbulent Heat And Fluid Flow In A Straight Square Duct At Higher Reynolds Numbers", Department of Building Services Engineering, The Hong Kong Polytechnic University, Kowloon, Hung Hom, Hong Kong, PR China, 2010.

[30] FLUENT, "FLUENT Guide – Chapter 10: Modeling Turbulence" Fluent Inc. November 28, 2001

[31] Suzuki, Y. and Kasagi, N. "Effects Of Noncircular Inlet On The Flow Structures In Turbulent Jets", Department of Mechanical Engineering, The University of Tokyo, Hongo, Japan, 2000.